Eur. Phys. J. E (2017) **40**: 105
DOI 10.1140/epje/i2017-11595-3

THE EUROPEAN PHYSICAL JOURNAL E

Regular Article

Entropy production in a fluid-solid system far from thermodynamic equilibrium*

Bong Jae Chung[1], Blas Ortega[2], and Ashwin Vaidya[2,a]

[1] Department of Bioengineering, George Mason University, Fairfax, VA 22030, USA
[2] Department of Mathematical Science, Montclair State University, Montclair, NJ 07043, USA

Received 31 July 2017 and Received in final form 24 October 2017
Published online: 24 November 2017 –

Abstract. The terminal orientation of a rigid body in a moving fluid is an example of a dissipative system, out of thermodynamic equilibrium and therefore a perfect testing ground for the validity of the maximum entropy production principle (MaxEP). Thus far, dynamical equations alone have been employed in studying the equilibrium states in fluid-solid interactions, but these are far too complex and become analytically intractable when inertial effects come into play. At that stage, our only recourse is to rely on numerical techniques which can be computationally expensive. In our past work, we have shown that the MaxEP is a reliable tool to help predict orientational equilibrium states of highly symmetric bodies such as cylinders, spheroids and toroidal bodies. The MaxEP correctly helps choose the stable equilibrium in these cases when the system is slightly out of thermodynamic equilibrium. In the current paper, we expand our analysis to examine i) bodies with fewer symmetries than previously reported, for instance, a half-ellipse and ii) when the system is far from thermodynamic equilibrium. Using two-dimensional numerical studies at Reynolds numbers ranging between 0 and 14, we examine the validity of the MaxEP. Our analysis of flow past a half-ellipse shows that overall the MaxEP is a good predictor of the equilibrium states but, in the special case of the half-ellipse with aspect ratio much greater than unity, the MaxEP is replaced by the Min-MaxEP, at higher Reynolds numbers when inertial effects come into play. Experiments in sedimentation tanks and with hinged bodies in a flow tank confirm these calculations.

1 Introduction

The classical work of Onsager [1,2] and Prigogine [3] on dissipative structures has revealed that self-organization of matter and energy is a fundamental characteristic of irreversible, physical systems. Irreversibility in nature is perhaps best captured by the laws of thermodynamics; the second law of thermodynamics and the extremum principle of entropy production proposed by Prigogine and Ziegler [4] provide great insight into emergent pattern formation in complex systems, out of thermodynamic equilibrium. The review paper by Martyushev [5] provides an excellent collection of examples of the use of the MaxEP in physics, chemistry and biology. Other arguments, such as the constructal theory, put forth by Bejan and collaborators [6] has shown thermodynamics to be a very powerful and fundamental theory of nature. However, we believe that some of the problems which have been studied so far are very complex making it rather difficult to gain insight into the workings of the MaxEP in conditions *far* from thermodynamic equilibrium. In this paper, we investigate the self-organization of a single rigid body, with orientational freedom, in a flowing Newtonian fluid. Some fundamental questions related to the MaxEP principle remain unanswered. One particularly significant question concerns the critical points where a system crosses over from a *near-equilibrium* state to *far from equilibrium*. Any discussion of the validity of the MaxEP as a meaningful guiding principle is therefore incomplete. To obtain a more systematic understanding of the validity of the MaxEP under various conditions, we take up a relatively simple toy problem of the orientation of a rigid body, immersed in a flow. Our previous work on this subject has shown MaxEP to be in agreement with other analytical, numerical and experimental work in the limit of very small Re[1]. The current paper extends our investigation to more complex cases and for higher Re which allows for a more thorough discussion of the above-mentioned issues.

* Contribution to the Topical Issue "Non-equilibrium processes in multicomponent and multiphase media" edited by Tatyana Lyubimova, Valentina Shevtsova, Fabrizio Croccolo.

[a] e-mail: vaidyaa@mail.montclair.edu

[1] The Reynolds number is defined as $Re = \frac{Ud}{\nu}$, where U is the uniform velocity, d is the characteristic length and ν is the kinematic viscosity.

Table 1. This table shows the properties of the rigid bodies used in our experiments. Here, δ refers to the maximum thickness of the body and d to the diameter.

Name	Shape	(δ, d)	Aspect ratio
S	Spheroid (3-dimension)	(1.27 cm, 2.54 cm)	0.5 ($\frac{\delta}{d}$)
$P1$	Half-ellipse (3-dimension)	(0.508 cm, 2.54 cm)	5.0 ($\frac{d}{\delta}$)
$P2$	Half-ellipse (2-dimension)	(0.508 cm, 2.54 cm)	5.0 ($\frac{d}{\delta}$)
$P3$	Half-ellipse (3-dimension)	(2.54 cm, 0.508 cm)	0.2 ($\frac{d}{\delta}$)
$P4$	Half-ellipse (2-dimension)	(2.54 cm, 0.508 cm)	0.2 ($\frac{d}{\delta}$)

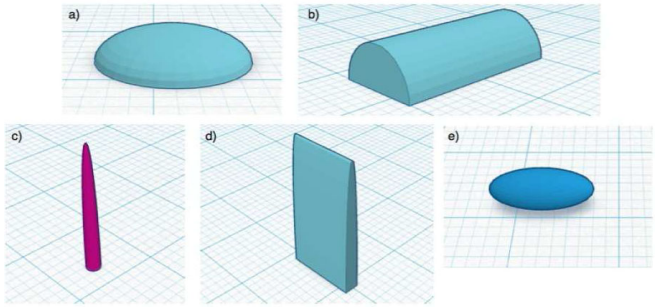

Fig. 1. The Tinkercad schematics for the different bodies used in our experiments. (a)–(d) refer to $P1$, $P2$, $P3$ and $P4$, respectively while (e) refers to S.

Symmetric bodies such as spheroids and cylinders, when introduced in a Newtonian fluid, orient themselves in a steady configuration such that their longer axis is perpendicular to the direction of the flow. This steady state depends upon the shape, size, density of the rigid body and the nature of the surrounding fluid [7,8]. In our earlier work on this subject, we analytically explained experimental observations concerning the terminal states of symmetric rigid bodies in Newtonian and non-Newtonian fluids at very small Reynolds numbers [9]. However, as the Re is increased, the fluid-solid system becomes highly nonlinear and the effect of inertia is seen to give rise to several bifurcations from the steady orientation to periodic oscillations [10,11] and beyond. Relevant experiments on terminal orientation have come in two forms: i) sedimentation, where the body falls through a quiescent fluid under gravitational force and as ii) a horizontal setup with the body being hinged at the center of a flow tank. In this latter case, the body is fixed in space, though allowed to rotate, while the fluid moves past it. Both types of experiments have been performed in our study and seen to be qualitatively similar. Therefore they will not be distinguished in this work.

The immense mathematical complexity of fluid-structure interaction (FSI) problems often demands a computational approach since analytical resolutions are not possible. While these methods effectively capture the dynamical process, they are computationally expensive and could be difficult to implement. The work of Onsager and Prigogine [1,3] in the early twentieth century shed some new light on taking a top-down, energy-based approach to problems in physics. It was realized that fluids are inherently dissipative systems and moving liquids are out of thermodynamic equilibrium allowing us to apply thermodynamic tools towards these problems. Constrained energy flows in non-equilibrium thermodynamic systems give rise to patterns in nature and can provide a valuable alternative to the Newtonian *force balance* approach. In this paper we apply the MaxEP principle to the problem of flow past a half-ellipse with two main objectives: O1) To test if the MaxEP is capable of explaining stable steady configurations for more complex shapes such as a half-ellipse, which possesses fewer symmetries than previously examined bodies. O2) To understand the nature of MaxEP states when the system is pushed far from thermodynamic equilibrium.

2 Experiments

Two types of experiments were performed. In the first, rigid half-ellipses of various dimensions were allowed to freely fall in a tank containing a viscous liquid. In the second experiment, the rigid bodies were hinged at the center of a water tunnel, allowing it to freely rotate about an axis, perpendicular to the flow. Several ellipsoids and half-ellipses made of PLA plastic, with aspect ratio[2] 5 and 0.2 were designed (using the software *Tinkercad*) and printed (see fig. 1) using a MakerBot Mini 3D printer. Refer to table 1 for a list of bodies used. Two- and three-dimensional half-ellipses were studied to compare with our two-dimensional numerical studies and to contrast with the three-dimensional case.

Sedimentation experiments

Spheroidal bodies and half-ellipses were released from rest in a glass tank with dimensions $60.96 \times 12.19 \times 12.19$ cubic cm containing about 6308 mL of a Newtonian liquid which was a mixture of water and corn syrup, in the ratio 3:2. The high viscosity of corn syrup was used to slow down the falling bodies and prevent them from moving too far into the oscillatory regime. Experiments were repeated several times, for different initial orientations of the body.

[2] The aspect ratio is defined by the ratio of the major axis to the semi-minor axis corresponding to disk-shaped objects and the ratio of the semi-major axis to the minor axis for elongated needle shaped bodies.

We observed that the spheroidal body, S, always oriented itself with its longer axis perpendicular to the direction of fall, as observed in previous work. The bodies $P1$ and $P2$ fell with their curved side pointing towards the direction of fall, which corresponds to an angle of 90°. $P3$ and $P4$ proved to be a little problematic to work with since they consistently moved towards the wall and slid down vertically giving us no information about their natural configuration under free fall. However, previous experiments on long, slender cylinders which are somewhat similar to $P3$ are insightful. It is observed [12] that slender needle-shaped bodies sedimenting in a viscous fluid, at low inertial regimes, tend to fall with their long axis perpendicular to the direction of gravity. In the case of body $P3$, the asymmetry of the ends would cause some minor deviation from this horizontal position due to the shift in the center of mass. However, as the aspect ratio increases to very large values, we would expect the body to fall precisely like the slender needle. The fall times of the bodies used were typically around 10 s to cover a height of 60.96 cm. Due to the slow speed of fall and relatively high viscosity, the particle Re in these experiments, assuming a characteristic length of 2.54 cm, was in the neighborhood of 0.012. In order to achieve higher Re, a modification of this experiment was performed which also avoided gravitational effects.

Experiments in flow tank

Alternatively, the experiment was also conducted in a flow tank containing water where the body was held at the center of a recirculating flow tank while the flow speed was varied to set the experiment at a specific Re. The flow speeds ranged from 1 cm/s to 10 cm/s allowing the Re to vary in the range $280 < Re < 2800$. In such experiments, the behavior of the solid body can be observed for long periods of time and exposed to higher values of Re compared to sedimentation studies. Previous studies have shown that experiments done in a flow tank reveal similar qualitative results to the sedimentation case with the only difference lying in the transition time to steady state which is accelerated by gravity. Studies on spheroids and cylinders of aspect ratios between 0.5 and 2.0 [11,13] have indicated that all bodies align, in their steady states, with their long axis perpendicular to the direction of the flow.

We performed similar experiments on half-ellipses $P1$ and $P3$ by suspending them at the center of a water tunnel (Engineering Laboratory Design Inc., Model 502) capable of flow rates between 0.1 and 1.0 fps at 0.37 kW. The dimensions of the test section of the water tunnel are $15.4 \times 15.4 \times 45.72$ cubic cm. The ellipse was hinged by means of a copper wire of thickness 0.023 cm passing through the center of mass of the body which was placed at the center of the tank in such a way as to prevent any translational motion. The orientation angle for all half-ellipses was defined such that the configuration where i) the curved side was up and flat side down, corresponded to $\theta = 0°$; ii) the curved side faced the flow, corresponded to $\theta = 90°$; iii) the flat side was up and curved side down, corresponded to $\theta = 180°$ and iv) the flat side faced the flow, corresponded to $\theta = 270°$ (see fig. 3(b)). $P1$ consistently showed $\theta = 0°$ and $\theta = 180°$ to be stable equilibria. The body turned to both of these configurations from rest and maintained these positions consistently for fairly high Re. $P3$ showed two stable states corresponding to $\theta = 90°$ and $\theta = 270°$ (see fig. 4(c)), with the former being more stable to perturbations than the latter. At $\theta = 270°$, the body starts to oscillate slightly at higher flow speeds and on occasion flips to $\theta = 90°$ when slightly disturbed.

3 Theoretical framework

The expression for entropy production for the case of a sedimenting body in a viscous fluid, has been shown to be of the functional form [13]

$$\begin{aligned}\mathcal{P} &= \frac{1}{T_0}\left(\int_\Omega \mathbf{T} : \mathbf{D}\,\mathrm{d}\Omega\right) - \frac{m_e}{T_0}\,\mathbf{g}\cdot\mathbf{U} \\ &= \frac{2\mu}{T_0}\left(\int_\Omega \mathbf{D} : \mathbf{D}\,\mathrm{d}\Omega\right) - \frac{m_e}{T_0}\,\mathbf{g}\cdot\mathbf{U}, \end{aligned} \tag{1}$$

where T_0 is the constant ambient temperature, $\mathbf{T}$ is the Cauchy stress tensor, $\mathbf{D}$ is the symmetric part of the velocity gradient $\mathbf{D} = \frac{1}{2}(\nabla\mathbf{u} + \nabla^T\mathbf{u})$, $\mathbf{u}$ is the fluid velocity field and $\mathbf{U}$ is the far-field velocity of the fluid as $\mathbf{x} \to \infty$. In the above equation, we decompose the stress tensor into $\mathbf{T} = -p\mathbf{I} + 2\mu\mathbf{D}$, p being the isotropic pressure and μ is the viscous coefficient. Also, $m_e = (\rho_b - \rho_f)|\mathcal{B}|$ is the effective mass, where $|\mathcal{B}|$ represents the volume of the body, ρ_b is the density of the body and ρ_f is the density of the fluid. The flow domain $\Omega = \Omega_0/\mathcal{B}$, where $\mathcal{B}$ is the region occupied by the rigid body and Ω_0 depends on the particular geometry of the problem. In the case of a freefalling body in an unbounded domain, $\Omega_0 = \mathbb{R}^3$. For the case of hinged body in a horizontal flow, the gravitational term can be neglected so the entropy production is identical to dissipation in the system [14,15].

The term $\mathcal{P}$ in eq. (1) contains the dissipation term as well the gravity term. The exchange of energy between kinetic and potential energies of the resulting fluid flow, introduced in our earlier paper [14] is shown to be an apt definition of the rate of entropy production, since it satisfies certain key conditions including: i) $\mathcal{P}$ must remain positive over the entire domain, ii) $\mathcal{P}$ must vanish when the Re tends to zero in the reversible, Stokes case and iii) $\mathcal{P}$ must satisfy Onsager's reciprocity relations.

We have previously shown [13] that for the problem of sedimentation of a rigid body of any shape in a Newtonian fluid at $Re = 0$, $\mathcal{P} = 0$. This is consistent with the balance of linear momentum and angular momentum equations [15] in the creeping motion regime and indicates that sedimentation, if slow enough, is a reversible process. In this case, the sedimenting body can fall with any orientation which is consistent with the experimental observations of Leal [7] on falling long bodies in a viscous fluid. If we restrict the geometry of the body to one possessing 3 planes of reflection symmetry and one axis of

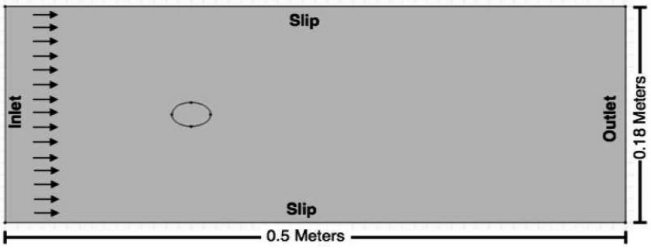

Fig. 2. A schematic of the computational domain with the elliptical body placed along the centerline of the channel.

rotational symmetry, such as in a prolate spheroid, then for $0 < Re \ll 1$ when inertial effects appear, $\mathcal{P} > 0$ and, in the reference frame of the body, we can write

$$T_0\,\mathcal{P} = U^2(K_{11}\cos\phi^2 + K_{22}\sin\phi^2) - m_e\mathbf{g}\cdot\mathbf{U}, \qquad (2)$$

where ϕ is the angle of orientation of the spheroid and K_{11}, K_{22} are positive coefficients pertaining to the drag coefficients of the spheroid in two different orientations. The derivative of $\mathcal{P}$ with respect to ϕ gives us

$$T_0\frac{\partial\mathcal{P}}{\partial\phi} = U^2(K_{22} - K_{11})\sin 2\phi \qquad (3)$$

yielding two possible extrema for $\mathcal{P}$, namely, $\phi = 0$ and $\phi = \pi/2$. Numerical computations for prolate spheroids indicate that $K_{22} > K_{11}$ [13], indicating that $\mathcal{P}$ has a maximum at $\phi = \pi/2$. This angle is known to coincide with the experimentally observed stable terminal state of the spheroid. This result is true for a variety of other bodies which belong to the same symmetry class, such as oblate spheroids, cylinders and torus [15]. The MaxEP principle therefore appears to serve as a selection principle to find the stable terminal configuration. Note that the gravity term does not really play a role in predicting the stable configuration but appears in the initial definition of the $\mathcal{P}$ to ensure the vanishing of entropy production in the limiting case of Stokes flow. Therefore, we could also attribute these results to the optimization of the dissipation function. The results obtained thus far can be summarized by the following proposition.

Proposition 1 ($Re \ll 1$). *Bodies possessing isotropic symmetry or containing three planes of reflection symmetry with one axis of rotational symmetry, align themselves such that their long axis is perpendicular to the uniform flow direction, in their terminal stable states. This configuration coincides with the state of maximum entropy production.*

4 Numerical simulations

Theoretical calculations restrict us to very small Re; in order to understand the effect of inertia on the system we resorted to two-dimensional numerical simulations using the software COMSOL Multi-physics [16]. We used the FSI module to simulate flow past an ellipse held in different orientations and for Re ranging from 1 to 14. Specifically, the entropy production in the entire domain and drag forces on the body were computed for a numerically generated flow, satisfying the Navier-Stokes, incompressibility and far-field equations

$$0 = \rho_f\left(\frac{\partial\mathbf{u}}{\partial t} + \mathbf{u}\cdot\nabla\mathbf{u}\right) - \mu\nabla\cdot(\nabla\mathbf{u} + \nabla^T\mathbf{u}) + \nabla p, \quad (4)$$

$$0 = \nabla\cdot\mathbf{u}, \quad (5)$$

$$\mathbf{U} = U\mathbf{e}_1 = \lim_{x\to\infty}\mathbf{u}. \quad (6)$$

As in eq. (1), in this case $\Omega = \Omega_0/\mathcal{B}$, where Ω_0 is the rectangular domain (18 cm × 50 cm) (see fig. 2). The body $\mathcal{B}$, which is an ellipse or half-ellipse in this problem, is placed along the centerline, at a distance of 15 cm from the entrance. The flow was subject to perfect slip conditions on the boundary to avoid the effect of boundary on the results. The net drag computed is given by

$$\mathbf{F}_D = \hat{u}\cdot\oint_S \mathbf{T}\cdot\hat{n}\,\mathrm{d}S = \underbrace{\hat{u}\cdot\oint_S -p\,\hat{n}\,\mathrm{d}S}_{\text{Pressure Drag}} + \underbrace{\hat{u}\cdot\oint_S 2\mu\,\mathbf{D}\cdot\hat{n}\,\mathrm{d}S}_{\text{Viscous Drag}}, \quad (7)$$

where $\hat{u}$ is a unit vector in the direction of flow and $\hat{n}$ is the outward unit normal to the surface S. The simulations for our study were performed on a two-dimensional domain with length 50 cm and height 18 cm. The channel inlet was set to be the front wall of the domain, at which a uniform inflow velocity was prescribed and the channel outlet was identified as the end wall of the domain, at which zero pressure, no viscous stresses were prescribed. The far-field condition as $x \to \infty$ is given by eq. (6). The top and bottom walls of the domain were set to have slip boundary conditions in order to suppress the influence of wall on the entropy production. The bodies were each fixed about a third of the channel length from the inlet and two thirds of the channel length from the outlet along the centerline (9 cm from the bottom) to avoid possible numerical inlet and outlet effects at the low Re explored here.

We used COMSOL (finite-element method) to generate about 8600 triangular mesh elements for all the simulations by using a "fine mesh". The flow speeds were chosen in the range 2 cm/s–50 cm/s and the kinematic viscosity, ν, was set to be 10 cm^2/s to achieve the desired Re. Convergence tests for this code have been reported in previous works [17, 18]. The time-dependent Navier-Stokes equations for the flow past the body were solved by the FSI module in COMSOL, which uses the PARADISO solver, which was run for 5 seconds in increments of 0.01 seconds. The end time was chosen to go well beyond the transient phase, well into the steady state. Flow past an ellipse and half-ellipse with different aspect ratios between 0.1 and 5 (namely 0.1, 0.25, 0.5, 1.0, 2.0, 3.0, 4.0 and 5.0) were studied. The ellipse was used as a benchmark to ensure that the numerical results coincided with previous theoretical predictions. Also, numerics allowed us to extend the scope of the work to higher Re, past the development of wake effects. As explained in the introduction, the half-ellipses

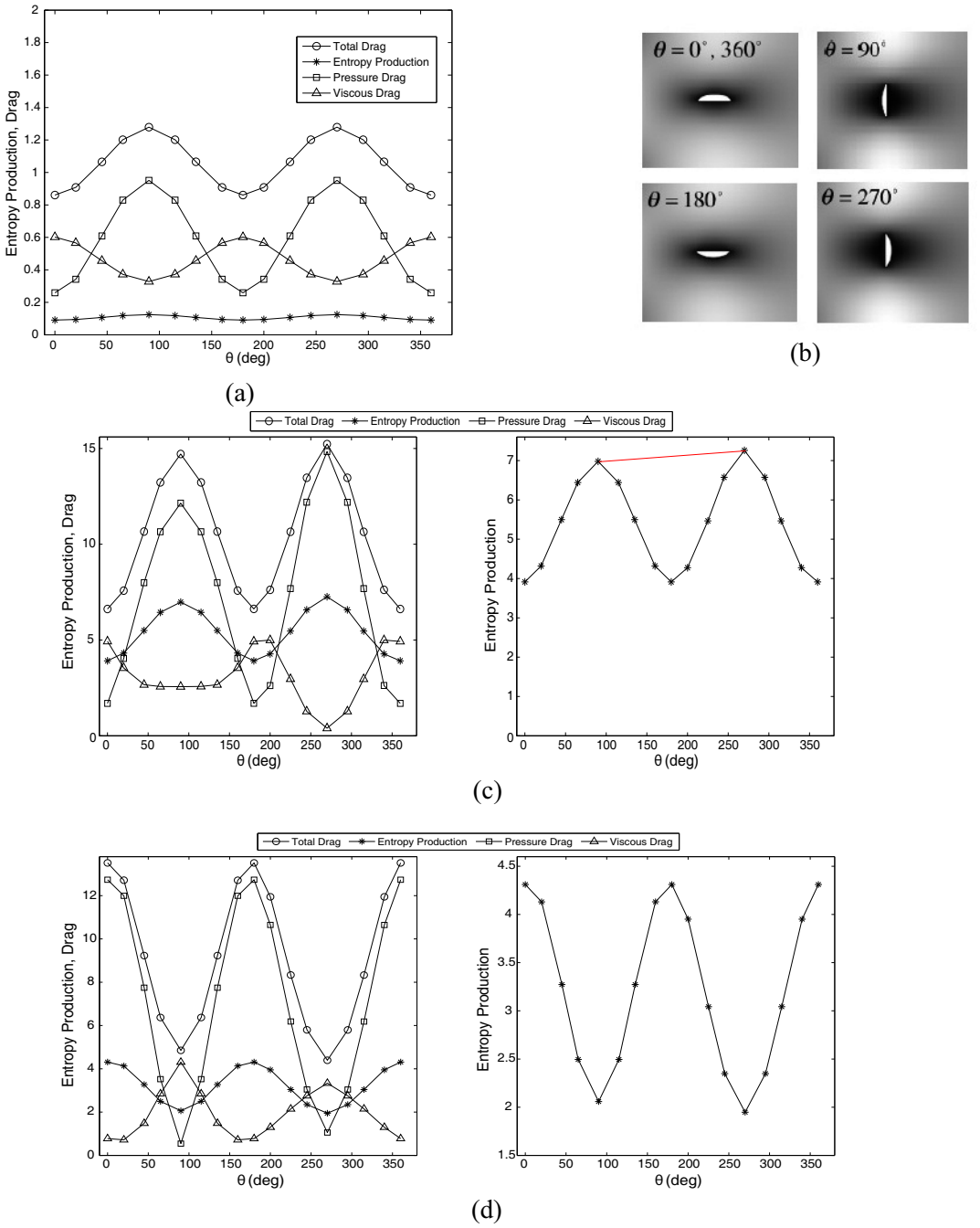

Fig. 3. Entropy production, drag force, pressure drag and viscous drag as a function of different orientation angles for (a) ellipse at $Re = 8$, (c) half-ellipse of aspect ratio 5 at $Re = 8$ and (d) half-ellipse of aspect ratio 0.1 at $Re = 6$. Panel (b) schematically depicts the various equilibrium orientation angles for the sample case of aspect ratio 5.

introduce added complexity to the problem by reducing the symmetry and allowing us to test the validity of the MaxEP in this new scenario. In addition to the aspect ratio, we also conducted a parametric sweep in Re and the orientation angle, θ, of the ellipse/half-ellipse, where the orientation of the body was changed around the center of mass of the half-ellipse. Figure 3(d) shows some sample cases of how θ was defined here. In our study, the Re took the values 0.02, 0.06, 0.1, 0.16, 0.2, 0.4, 0.8, 1, 1.2, 1.6, 2, 4, 6, 8, 10 and 14, while θ ranged from 20°, 45°, 65°, 90°, 115°, 135°, 160°, 180°, 200°, 225°, 245°, 270°, 295°, 315°, 340°, to 360°.

Case 1: Flow past ellipse for $0 < \mathrm{Re} < 10$

We began testing the validity of the MaxEP as a pattern selection principle in a Newtonian fluid by running our simulation with the very well-known case of an ellipse. It is theoretically proven for $Re \ll 1$ that bodies with fore-

aft symmetry assume a stable orientation such that the longer axis becomes perpendicular to the direction of the flow. The ellipse was chosen, without loss of generality, to have dimensions 0.02 m (major axis) and 0.0078 m (minor axis). Figure 3(a) shows two angles corresponding to the MaxEP states, namely $\theta = 90°$ and $\theta = 270°$, which are indistinguishable positions with respect to the incoming flow. The results of our numerical study show that the terminal steady angle coincides with the configuration of maximum entropy production and is in agreement with previous experimental observations. Overall, we can summarize our results by means of the following proposition.

Proposition 2 ($0 < Re < 10$). *Bodies possessing isotropic symmetry or containing three planes of reflection symmetry with one axis of rotational symmetry align themselves such as their long axis is perpendicular to the uniform flow direction, in their terminal stable states. This configuration coincides with i) the maximum entropy production, ii) the maximum total drag, iii) the maximum pressure drag and iv) the minimum viscous drag.*

Case 2: Half-ellipse of aspect ratio $\gg 1$

Numerical computation of entropy production for the flow past a half-ellipse was performed for Reynolds numbers $0 < Re \leq 10$. In the estimation of the Re, d was chosen to be twice the major axis. Let us define a set $\mathcal{S}$ which contains the maxima of $\mathcal{P}$. In the case of the half-ellipse, $\mathcal{S}$ contains two local maxima, at 90° and 270° (see fig. 3(c)), the former of which is the experimentally observed stable configuration for reasonably large Re at which the flow remains steady; there is no study yet in the very small Re regime for such a body. Drawing from the observations of spheroidal bodies which maintain the same stable steady state, we will assume that the half-ellipse preserves its steady stable configuration of 90° for $0 < Re < 10$. Our calculations reveal that the total drag force and pressure drag, also reveal multiple extrema at these angles.

How, then, do we choose the stable state from set $\mathcal{S}$? Propositions 1, 2 do not help since the ellipse possesses only one extremum. To formulate the appropriate, more general selection principle, we examined the entropy production for the two extremum angles as a function of Re. Figure 4(a) shows the entropy production *versus* Re for a half-ellipse of aspect ratio 5 which reveals two distinct phases: in Phase 1, corresponding to $Re < 1.6$ (approximately), the stable state (90°) appears to correspond to max $\mathcal{S}$ (where the difference between the two entropy production extrema is extremely small), while in Phase 2, the stable state switches to min $\mathcal{S}$ (see the right panel of fig. 3(c)). As the flow speed increases and pushes the system farther away from thermodynamic equilibrium, the selection principle appears to reveal more complexity. In summary:

Proposition 3 ($0 < Re \leq 10$). *In the near equilibrium state, corresponding to $0 < Re \leq 1.6$, half-ellipse possessing one axis of reflection symmetry, such as half-ellipses, with sufficiently large aspect ratio, reveal equilibria when their flat or curved sides become perpendicular to the uniform flow direction, corresponding to orientation angles 90° and 270°. Both configurations are quantitatively similar. Assuming that the stable configuration corresponds to the angle of 90°, this case coincides with i) the maximum entropy production; ii) the maximum total drag; iii) the min-max of pressure drag and iv) the max-min of viscous drag, over all angles. When the system is sufficiently far from thermodynamic equilibrium, corresponding to $1.6 < Re \leq 10$, the stable configuration of 90° coincides with i) the min-max of entropy production; ii) the min-max total drag; iii) the min-max of pressure drag and iv) the max-min of viscous drag.*

Note that the upper limit of Re shown in Phase 2 and reported in this paper is limited by the range of flow speeds explored studied here and is not an indication of the limits imposed by thermodynamic effects.

Case 3: Half-ellipse of aspect ratio $\ll 1$

For the half-ellipse of aspect ratio $\ll 1$, we considered dimensions of 0.028 m (semi-major axis) and 0.0028 m (minor axis) resulting in $AR = 0.1$. Our simulations reveal that, in this case, the MaxEP states occur at the angles $\theta = 0°$ and 180° (see fig. 3(d)). These are indistinguishable positions with respect to the direction of the flow and persist for $Re \leq 14$ where our computation concluded as seen in fig. 4(b). The more symmetric nature of this body around its longer axis changes the equilibrium position and the results observed here are similar to what might be observed for a long ellipse. In summary:

Proposition 4 ($0 < Re \leq 14$). *A half-ellipse, with its minor axis much shorter that its semi-major axis, will orient itself such that the longer axis is perpendicular to the direction of the flow, i.e. $\theta = 0°$ or 180°. This position coincides with i) the maximum entropy production, ii) the maximum total drag, iii) the maximum pressure drag and iv) the minimum viscous drag.*

5 Discussion

In summary, our numerical computations of entropy production indicate that, as in the case of symmetric spheroidal bodies, half-ellipses also adopt the MaxEP state in a flow for their equilibrium angle. In the case when there is only one equilibrium this is the stable angle as well. Bodies with aspect ratios much greater than unity display more a complex behavior since they possess two equilibria. In this particular case, it is the min-max of EP which is the more stable configuration when the system is far from equilibrium (*i.e.*, $Re > 1.6$). These predictions are also confirmed by previous and current experimental work. The current work treats only the cases of aspect ratios which are much greater or less than unity. Our study shows that half-ellipses of aspect ratio 3 and above behave

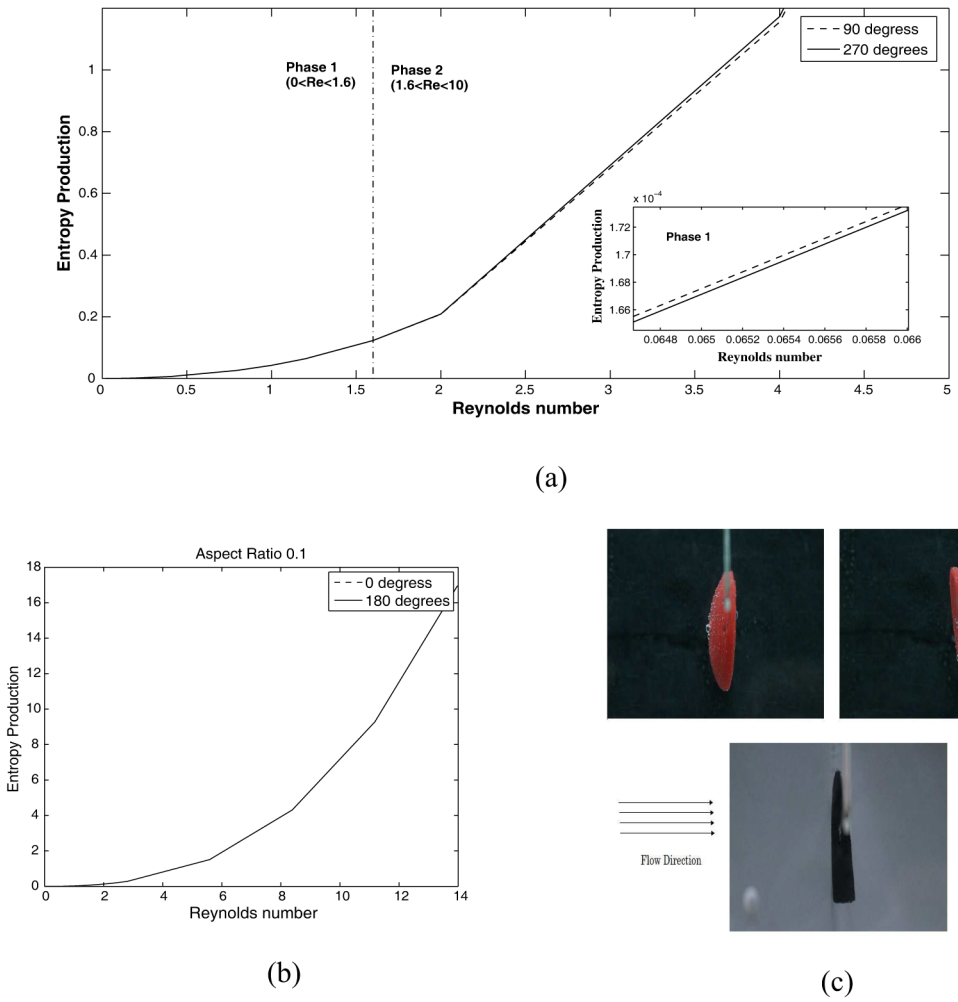

Fig. 4. Panel (a) shows the entropy production *versus* Re for the case of $\theta = 90^\circ$ and $\theta = 270^\circ$. The boundary between phase 1 and 2 (at $Re = 1.6$) is determined based on the observation switching of maxima in our data. Panel (b) shows a similar graph for the angles 0° and 180°, corresponding to half-ellipse of aspect ratio 0.1. Panel (c) shows the experimentally observed equilibria for the two half-ellipses.

in a similar manner, while bodies with aspect ratio below 0.25 yield identical results. Our numerical calculations for aspect ratio 0.5, 1 and 2 seems to suggest these to be far more complicated systems with intermediate extremal states, *i.e.* between 0° and 90°. These results need to be confirmed with very careful experimentation. Our initial hypothesis is that there must be a continuous transition in the stable configuration as the aspect ratio is changed. We hope to report the results on these systems in our future work.

While there is not much in the literature dealing with half-ellipses [19–21], the work on orientation of symmetric and asymmetric dumbbells by Candelier and Mehlig [19] deserves some comments. This theoretical treatment uses the method of reflections to investigate the torques that induce terminal orientation of a long, slender dumbbell. The authors find that the symmetric dumbbell falls horizontally, *i.e.* with the central axis (massless in their case) perpendicular to the direction of fall. However, even a small asymmetry between the two spheres gives rise to an additional torque imposed by the inhomogeneous mass distribution causing the body to fall with its heavier (bigger) side down. Our current and previous work [15] shows that symmetric bodies with fore-aft symmetry and three planes of reflection, such as the symmetric dumbbell, should fall with their long axis perpendicular to gravity, as also is the case with symmetric cylinders or spheroids. This case is in agreement with the results of Candelier and Mehlig. However, the asymmetric cases of the dumbbell and half-ellipse do not match as well and are not that easy to compare, perhaps due to more nuanced reasons which might be related to the specific differences in geometry, inertial effects and mass distribution. The take-away message from these studies is that the effect of symmetry breaking results in interesting and significant deviations from the symmetric cases and need to be examined in greater detail.

One other significant outcome of this approach in general is the agreement between the entropy-based optimization and the mechanical arguments. This connection is in fact what has drawn attention to the MaxEP approach in

climate modeling, ecology and so many other areas where it has been successful [5,22]. Perhaps we should not be so surprised about this connection since it is highly plausible that the patterns revealed by forces and torques could have their origins somewhere in the energetics (or "entropics") of the problem. In an earlier work [23], we have shown that the derivative of $\mathcal{P}$ with respect to translational and angular velocity yields the Stokesian forces and torques on a body. Also, we have consistently shown in all our work in dealing with dissipative systems like fluid-solid interaction that the optimization of $\mathcal{P}$ with respect to the right order parameter [14] reveals the correct experimentally observed pattern. As of now, there is no rigorous, first-principle–based proof of why this works so well but this remains a significant problem for future investigation.

Therefore, in answer to question O1 stated in the introduction, the MaxEP principle appears to continue to describe the steady states for a large class of bodies immersed in a flow. For the stable state, it appears that the Min-MaxEP is the correct selection principle for bodies possessing orthotropic symmetry and 2 planes of symmetry. Whether this is the most general principle or a projection of something more complex remains to be seen. One of the most pressing issues related to the MaxEP is its validity in far-from-equilibrium situations, which is our second objective O2. In fact, while the very definition of "far from equilibrium" is unclear in general, the advantage of this particular problem in fluid mechanics is that it is capable of shedding some light on this important issue since much is known about critical flow bifurcations [24]. Computations presented here show that in the regime of slow flows defined by $Re \leq 1.6$, MaxEP holds for all the bodies studied. However, for $1.6 < Re < 10$, inertial effects become prominent and the MaxEP is replaced by the Min-MaxEP. The studies conducted so far appear to indicate that as the flow becomes sufficiently fast to produce prominent inertial effects, multiple equilibria are produced with the Min-Max corresponding to the most stable pattern. Based on experiments we can expect these results to hold for much higher Re as long as the steady wake persists. The MaxEP can be bolstered by additional constraints to serve as a valid selection principle. Propositions 2–4 reveal that the pressure or viscous drag are also uniform predictors of the steady state and the *min-max of pressure drag* or *max-min of viscous drag* can also work as a selection principle for bodies with one axis of symmetry. The shift in the entropy production beyond $Re \approx 1.6$ coincides with the critical regime where flow separation is thought to occur and wake vortices become more prominent [24] in the flow past a cylinder. Interestingly, the same critical Re also shows up in our thermodynamic analysis of flow past a half-ellipse. This change is also similar to the results by Hubler *et al.* [25] on the entropy production during the self-assembly of nanotubes where the authors observe a switching from a maximum to a minimum entropy production with increasing dissipative effects.

Other than shedding light on the two issues addressed above, the importance of this work lies in its potential to address some very deep philosophical and biological problems. Recent work in the area of ecological psychology [26,27] argues that dissipative structures are inherent properties of living and certain non-living systems. Therefore, the end-directedness of the physical systems treated in this paper could potentially shed light on the goal-oriented behavior of living systems. The problem treated here provides another example of an end-directed system whereby the flow of energy in out-of-thermodynamic-equilibrium states forces the rigid body to organize itself in a specific configuration determined by the extremum or increase of entropy production. We have argued at length in a previous work [14] that reliance on the MaxEP is not immediately indicative of teleology; the same outcome can also be predicted by a torque balance argument [9]. Also, the fact that the stable states in our example are characterized by the extremum of drag and entropy production points to a very fundamental, underlying connection between the two ways of talking about natural laws. This makes the effectiveness of the entropy production argument an even more fundamental mystery that deserves continued attention.

The flow tank experiments in the current study are incapable of achieving the low Re limit explored in the computations due to technical difficulty of having flow control at low pressures. As a result the low Re experiments were performed in a modified sedimentation tank. However, despite the relatively high flow speeds and Re in our experiments, the stable configuration of the rigid body is still aligned with theoretical predictions. Elaborate experiments across the same range of Re as in the numerical study need to be performed in the future; these and other shortcomings of our current work will be dealt with in our future studies. We also plan on examining the validity of the MaxEP and variations thereof for various other classes of bodies, including half-ellipses with aspect ratios close to 1 and those with fewer symmetry planes than the ones explored here

All authors contributed equally to the work. BJC and AV designed the study and helped in writing the paper. BO performed the numerical study and also performed some of the experiments discussed here with AV. The authors would like to thank Dr. Steven Greenstein for his help with 3D printing.

References

1. Lars Onsager, Phys. Rev. **37**, 405 (1931).
2. Lars Onsager, Phys. Rev. **38**, 2265 (1931).
3. Ilya Prigogine, *Introduction to Thermodynamics of Irreversible Processes*, 3rd edition (Interscience, New York, 1967) p. 1.
4. Hans Ziegler, *An Introduction to Thermomechanics*, Vol. **21** (Elsevier, 2012).
5. L.M. Martyushev, V.D. Seleznev, Phys. Rep. **426**, 1 (2006).
6. Adrian Bejan, Sylvie Lorente, Phys. Life Rev. **8**, 209 (2011).
7. L.G. Leal, Annu. Rev. Fluid Mech. **12**, 435 (1980).
8. Yaoqi Joe Liu, Daniel D. Joseph, J. Fluid Mech. **255**, 565 (1993).

9. Giovanni P. Galdi, Handb. Math. Fluid Dyn. **1**, 653 (2002).
10. Roberto Camassa *et al.*, *Vortex induced oscillations of cylinders at low and intermediate Reynolds numbers*, in *Advances in Mathematical Fluid Mechanics* (Springer, Berlin Heidelberg, 2010) pp. 135–145.
11. B. Chung *et al.*, Arch. Appl. Mech. **86**, 627 (2016).
12. R.E. Khayat, R.G. Cox, J. Fluid Mech. **209**, 435 (1989).
13. Bong Jae Chung, Ashwin Vaidya, Physica D: Nonlinear Phenom. **237**, 2945 (2008).
14. Bong Jae Chung, Kirk McDermid, Ashwin Vaidya, Eur. Phys. J. B **87**, 20 (2014).
15. Bong Jae Chung, Ashwin Vaidya, Appl. Math. Comput. **218**, 3451 (2011).
16. `https://www.comsol.com/`.
17. Ryan Allaire *et al.*, Int. J. Non-Linear Mech. **69**, 157 (2015).
18. Bogdan Nita, Peter Nolan, Ashwin Vaidya, Comput. Appl. Math. **36**, 1733 (2017).
19. F. Candelier, B. Mehlig, J. Fluid Mech. **802**, 174 (2016).
20. J. Einarsson *et al.*, Phys. Fluids **28**, 013302 (2016).
21. Greg A. Voth, Alfredo Soldati, Annu. Rev. Fluid Mech. **49**, 249 (2017).
22. Ichiro Aoki, Ecol. Complex. **3**, 56 (2006).
23. Ashwin Vaidya, *MaxEP and Stable Configurations in Fluid-Solid Interactions*, in *Beyond the Second Law* (Springer Berlin, Heidelberg, 2014) pp. 257–276.
24. M.M. Zdravkovich, J. Fluid Mech. **350**, 377 (1997).
25. Alfred Hubler, Andrey Belkin, Alexey Bezryadin, Complexity **20**, 8 (2015).
26. Tehran J. Davis *et al.*, Ecol. Psychol. **28**, 23 (2016).
27. Dilip Kondepudi, Bruce Kay, James Dixon, Phys. Rev. E **91**, 050902 (2015).